Gómez Jiménez, MD.; Fuster Almunia, C.; Ocaña-Cuesta, J.; Alonso, J.; Perez Amador, MA. (2019). RGL2 controls flower development, ovule number and fertility in Arabidopsis. Plant Science. 281:82-92. https://doi.org/10.1016/j.plantsci.2019.01.014

Title: RGL2 controls flower development, ovule number and fertility in Arabidopsis

Authors: María Dolores Gómez, Clara Fuster-Almunia, Javier Ocaña-Cuesta, Jose M Alonso, Miguel A Pérez-Amador

PII: S0168-9452(18)31148-8
DOI: https://doi.org/10.1016/j.plantsci.2019.01.014
Reference: PSL 10052

To appear in: *Plant Science*

Received date: 19 September 2018
Revised date: 16 October 2018
Accepted date: 12 January 2019

Please cite this article as: Gómez MD, Fuster-Almunia C, Ocaña-Cuesta J, Alonso JM, A Pérez-Amador M, RGL2 controls flower development, ovule number and fertility in Arabidopsis, *Plant Science* (2019), https://doi.org/10.1016/j.plantsci.2019.01.014

RGL2 controls flower development, ovule number and fertility in Arabidopsis

María Dolores Gómez[1], Clara Fuster-Almunia[1]; Javier Ocaña-Cuesta[1], Jose M Alonso[2], and Miguel A Pérez-Amador[1]*

[1]Instituto de Biología Molecular y Celular de Plantas (IBMCP), Universidad Politécnica de Valencia (UPV)-Consejo Superior de Investigaciones Científicas (CSIC). Ciudad Politécnica de la Innovación, Ed. 8E, Ingeniero Fausto Elio s/n, 46022 Valencia, Spain.

[2]Department of Plant and Microbial Biology, Program in Genetics, North Carolina State University, Raleigh, North Carolina 27695, USA.

*Corresponding author:

Miguel A. Perez-Amador (mpereza@ibmcp.upv.es).

Instituto de Biología Molecular y Celular de Plantas (IBMCP), Universidad Politécnica de Valencia-Consejo Superior de Investigaciones Científicas (CSIC). Ingeniero Fausto Elio s/n, 46022 Valencia, Spain. Phone +34-963877872

Highlights

- Genetic tools have been generated to study RGL2 expression and function through plant development
- 2. RGL2 has a role in flower development and ovule initiation
- 3. Gain-of-function of RGL2 alters flower development, but increases ovule number

Abstract

DELLA proteins are a group of plant specific GRAS proteins of transcriptional regulators that have a key role in gibberellin (GA) signaling. In *Arabidopsis*, the DELLA family is formed by five members. The complexity of this gene family raises the question on whether single DELLA proteins have specific or overlapping functions in the control of several GA-dependent developmental processes. To better understand the roles played by RGL2, one of the DELLA proteins in *Arabidopsis*, two transgenic lines that express fusion proteins of Venus-RGL2 and a dominant version of RGL2, YPet-rgl2Δ17, were generated by recombineering strategy using a genomic clone that contained the *RGL2* gene. The dominant YPet-rgl2Δ17 protein is not degraded by GAs, and therefore it blocks the RGL2-dependent GA signaling and hence RGL2-dependent development. The RGL2 role in seed germination was further confirmed using these genetic tools, while new functions of RGL2 in plant development were uncovered. RGL2 has a clear function in the regulation of flower development, particularly stamen growth and anther dehiscence, which has a great impact in fertility. Moreover, the increased ovule number in the *YPet-rgl2Δ17* line points out the role of RGL2 in the determination of ovule number.

Abbreviations

GA, gibberellin, PCB, paclobutrazol, L*er*, Landsberg *erecta*.

Keywords

Gibberellin, DELLA, RGL2, Arabidopsis, development, ovule

1. Introduction

Plants compensate for their immobility by their ability to perceive environmental signals and respond to them with changes in their structure and physiology, thus ensuring their survival and reproduction. Plant hormones regulate endogenous development processes and, in addition, integrate external signals and orchestrate adaptive responses to abiotic and biotic stresses. One of these hormones are the gibberellins (GAs) that together with the DELLA proteins constitute a mechanism that integrates environmental and development signals [1-3].

GAs are tetracyclic diterpenoids that participate in the control of key developmental processes throughout the plant life cycle, from seed germination, to leaf expansion, stem and root elongation, flowering time, flower development, or fruit and ovule development [4-7]. The molecular mechanism of GA action lies in three major modules: (1) GA synthesis, (2) the GA signaling core, which includes the GA receptors GID1 and the DELLA proteins, and (3) DELLA-dependent changes in gene transcription mediated by the direct protein-protein interaction of DELLA with several transcription factors [8-10].

Upon binding to the bioactive GA, the GID1 receptor suffers a conformational change that allows the binding of the DELLA protein. The complex GA-GID1-DELLA is then recognized by the $SCF^{SLY1/GID2}$ ubiquitin E3 ligase complex for poly-ubiquitination and degradation by the 26S proteasome of the DELLA protein. This way, reduced GA concentration promotes the accumulation of DELLA proteins that repress GA responses, in return when GA concentration increase, DELLA proteins are degraded, leading to the activation of GA responses [2].

DELLA proteins are a subfamily within plant specific GRAS family of transcription regulators. As GRAS proteins, DELLAs present a conserved C-terminal domain that is involved in protein–protein interaction and transcriptional regulation that

is formed by two leucine heptad repeats (LHRI and LHRII) and three conserved motifs (VHIID, PFYRE and SAW). Unlike other GRAS proteins, DELLA proteins have an N-terminal domain with two conserved domains: the DELLA domain (with conserved amino acid sequence Asp-Glu-Leu-Leu-Ala, origin of the name DELLA) and the TVHYNP domain. Mutations in the DELLA or TVHYNP domains prevent the interaction of the protein with the GID1 receptor, which stabilizes the DELLA protein, giving rise to a plant with a semi-dominant GA-insensitive dwarf phenotype [2,11,12]. On the contrary, null mutations in *DELLA* genes lead to constitutive GA response, which resembles the phenotypes of GA-treated plants. At the molecular level, GA-signaling repressors DELLA proteins act as putative transcriptional regulators. They are nuclear-localized proteins that lack a canonical DNA binding domain, but bind to a larger range of proteins, mostly transcription factors, modulating their transcriptional function [1,2]. Uncovering the nature of the DELLA interactor proteins has paved the road to a true understanding of the molecular mechanism by which the DELLA proteins regulate GA responses, integrating endogenous and external signals to coordinate growth, development and stress responses [1-3].

Most major families of plants encode one or two *DELLA* genes [1]. An interesting scenario raises in the model plant *Arabidopsis thaliana*, with 5 DELLA proteins encoded in its genome: GAI (GA-INSENSITIVE, At1g14920), RGA (REPRESSOR OF GA1-3, At2g01570), and the three RGA-LIKE, RGL1 (At1g66350), RGL2 (At3g03450), and RGL3 (At5g17490).What is the biological significance of the *DELLA* gene redundancy in *Arabidopsis*? Do DELLA proteins play overlapping roles in development? Or, on the contrary, do they play specific roles? A great progress was achieved in the past to address the question of genetic redundancy in *Arabidopsis* and to assign particular functions to each DELLA protein in plant growth and development

and in the stress response. A widely used approach to study DELLA function is the characterization of null *DELLA* mutants in the strong GA deficient mutant *ga1* background [13,14]. Deficiency of GAs in *ga1* leads to strong accumulation of DELLA proteins, blocking GA responses. By sequentially removing DELLA proteins in single and multiple loss-of-function *DELLA* mutants, the different processes controlled by these particular DELLAs can be uncovered. Therefore, the characterization of the phenotypes of the null mutant combinations of these 5 genes in the *ga1* background, along with the data gathered using the dominant version of GAI and RGA, in the *gai-1* mutant and the *pRGA:GFP-rgaD17* line, respectively, allowed for the dissection of specific roles each of these proteins play in *Arabidopsis* development and stress response. For example, RGA is a major player in the GA-mediated control of stem growth, trichome initiation, flowering time and apical dominance [13]. GAI and RGA act synergistically as major repressors of vegetative growth and floral initiation [15,16]. RGL2, along with RGL1, has a major role in the GA-mediated seed germination [17,18]. RGA, along with RGL1 and RGL2, controls petal and sepal development, stamen filament length, microsporogenesis, and male fertility [18,19]. Finally, GAI, RGA, RGL1 and RGL2 regulate ovule integument development and fruit development [6,7,20,21]. In contrast, RGL3 performs a minor function in plant development processes, but act as a positive regulator in the defense response [22,23]. All these evidences indicate that the DELLA proteins play specific but also redundant roles. By means of *RGA-RGL2* promoter switching, Gallego-Bartolome et al. [24] proposed that functional diversification of DELLA proteins rely mainly on changes in their gene expression patterns rather than on their molecular function, as both proteins can interact with similar molecular partners. Thus, temporal and spatial expression patterns of the different DELLA proteins may account for their roles through the plant life cycle.

As mentioned, RGL2 participates in flower development including ovule integument growth [6,18,19]. RGL2 is mainly known for being the major DELLA in GA-dependent seed germination. Thus, germination of the *ga1* seeds is released by loss-of-function of *RGL2* in the *rgl2-1* mutant [17,18]. In addition, constitutive expression of *RGL2* reduced seed germination [25]. All these data indicate that RGL2 is a negative regulator of the GA-mediated seed germination in *Arabidopsis*.

To take a closer look at the role of RGL2 function in plant development, the *pRGL2:YPet-rgl2Δ17* transgenic line was generated and characterized. It expresses a dominant version of the protein RGL2, equivalent to that of GAI and RGA in *gai-1* and *GFP-rgaΔ17*, under the control of its endogenous promoter and fused to the fluorescent protein *YPet*. In addition, the *pRGL2:Venus-RGL2* line that expresses the GA-degradable version of RGL2 was also created. These lines were used to determine both the defects in plant development caused by stable RGL2 protein, and to follow expression of the endogenous gene. The data obtained reveal a major role of RGL2, not only in seed germination, but also in the growth and development of floral organs, mainly petal and stamen, as well as anther dehiscence. Moreover, RGL2 participates in the control ovule initiation, promoting the formation of more ovules per pistil with no alterations of pistil length. On the contrary, RGL2 seems not to play a significant role in the regulation of flowering time, plant architecture or height. This study contributes to a better understanding of the specific roles of this DELLA protein in the development of *Arabidopsis*, and provides useful tools for further investigations.

2. Materials and Methods

2.1. Plant material

The *Arabidopsis thaliana* plants used were in the Landsberg *erecta* (L*er*) genetic background. Single *rgl2-1* mutant was obtained from the Nottingham Arabidopsis Stock Center (www.arabidopsis.info). Genotyping was carried out using oligos listed in Supplemental Table S1. Seeds were surface-sterilized in EtOH and plated onto ½ MS media plates [26] supplemented, in accordance with each experiment, with 5 µM glufosinate to select transgenic plants, 1 µM paclobutrazol (PCB) to inhibit GA-dependent germination or 2 µM to induce DELLA stabilization in seedlings, or 1-3 µM GA_{4+7} to induce DELLA degradation in seedlings. Plates were kept at 4°C in darkness for four days, and were transferred to a growth chamber at 22°C in long day photoperiod (16/8h) for ten days. Seedlings were then transferred to soil (a mixture of peat moss, vermiculite and perlite, 2:1:1) and grown to maturity in a growth chamber at 22°C in long day photoperiod (16/8h).

2.2. Fertility assay, and measurement of plant height and floral organs

Fertility was scored from hand pollinated flowers. Flower buds of L*er* or *pRGL2:YPet-rgl2Δ17* plants were first emasculated one day before anthesis and pistils were pollinated the next day with either L*er* or *pRGL2:YPet-rgl2Δ17* pollen. In all cases, fruits were collected at maturity (14-18 dpa) and seed number and silique length was measured. GA response of the pistils was assayed by the application of GA_{4+7} to unfertilized pistils. For this, flowers were emasculated one day before anthesis and treated the next day with 300 µM GA_{4+7} (Fluka) and 0.02% (v/v) Tween 80, pH 7.0. Fruits were harvested 12 days after treatment, and scanned to measure final length with ImageJ software [27]. Plant height was scored by measuring the length of the main inflorescence stem one week after bolting. Length of the four floral four whorls were

measured from early and late flowers, by dissecting the flower under a stereomicroscope, photographed and analyzed with ImageJ software. Experiments were repeated three times with similar results.

2.3. Pollen germination assay

For the *in vitro* analysis of pollen germination and pollen tube growth, pollen was harvested from flowers at anthesis (one flower per plant from 25 individual plants for each genotype). Pollen was germinated on solid pollen germination medium consisting of 5 mM $CaCl_2$, 1 mM $MgSO_4$, 5 mM $CaCl_2$, 0.01% H_3BO_3, and 10% (w/v) sucrose. The pH was adjusted at 7.5 and media was solidified with 1.5% low-melting agarose. The plates were incubated at 24°C under moist conditions in the dark for 16h. A Nikon Eclipse E600 microscope was used to visualize pollen germination and pollen tube growth. The pollen tube length was measured using the NeuronJ plug-in of ImageJ software.

2.4. Construction of *pRGL2:Venus-RGL2 and pRGL2:YPet-rgl2Δ17*

Construction of a translational fusion Venus-RGL2 and the dominant version YPet-rgl2Δ17 were generated by bacterial homologous recombination technology (recombineering), using a modified version of the pBALU6 [28] and a *galK* counter-selection and/or Flp recombinase [29-31]. Both constructs were generated using the JAtY clone JAtY56P08 from the JIC (JAtY library at http://orders2.genome-enterprise.com/libraries/arabidopsis/jaty.html) in the pYLTAC17 vector [32]. The *RGL2* gene (*At3g03450*) was located between position 37.5 and 33.9 kb of the 73 kb genomic fragment of JAtY56P08. First, the JAtY clone was moved to SW102 or SW105 *E. coli* strain to allow recombineering with *galK* for *YPet-rgl2Δ17* or *galK/Flp*

for *Venus-RGL2*, respectively [30]. In all procedures, bacterial media were supplemented with 25 µg/mL kanamycin.

The Venus [28] and YPet [31] protein used as fluorescent markers were used to generate PCR products for recombineering as previously described [31]. All oligos used are listed in the Supplemental Table S1, and the general procedure is described in the supplemental Figure S1. Once generated, the constructs were used to transform a recA-deficient *Agrobacterium tumefaciends* GV3101 (pMP90) strain [31], to ensure integrity of modified JAtY clones. L*er Arabidopsis* plants were transformed by the floral dip method [33], and T1 seedlings were selected on MS media supplemented with 50 µg/mL of glufosinate in the presence of 500 µg/mL of vancomycin to limit the growth of any *Agrobacterium.* Homozygous lines were selected based on glufosinate resistance of the T3 progeny.

2.4.1. Construction of *pRGL2:Venus-RGL2*

For the introduction of Venus into the Nt of RGL2, a galK-FLP cassette in pBALU6 was used [28]. Flippation of the region between the FRT sequences was done by induction of the Flp recombinase with L-arabinose in the SW105 *E. coli* strain [30]. In addition, the Venus-FRT-galK-FRT cassette was flanked by universal 5' and 3' adaptor sequences (Supplemental Table S1). The *galK* gene in the recombineering cassette is used as a positive selectable marker in the presence of galactose and as a counter-selectable marker in the presence of 2-deoxygalactose [31]. First, a PCR was carried out with recombineering oligos RGL2-Nt_RF and RGL2-Nt_RR using the Venus-FRT-galK-FRT cassette as template, and Accuzyme proofreading Taq DNA polymerase (Bioline). These oligos have a 50 bp sequence homolog to the upstream and downstream region from the ATG of *RGL2*, followed at 3' by the universal adaptor

sequence. Original clone JAtY56P08 was first introduced in SW105 [30]. The PCR product was introduced in heat-induced SW105 cells bearing the JAtY56P08 clone by electroporation, and positive colonies were selected in M9 minimal media supplemented with 0.2% of galactose as carbon source. After selection, removal of the *galK* marker was carried out by a short incubation in 0.1% L-arabinose, and selection of the clones in minimal media supplemented with 0.2% 2-deoxygalactose. In all steps, the constructs were tested by PCR and sequencing. See supplemental Figure S1A for details.

2.4.2. Construction of DELLA deletion in RGL2 to generate *pRGL2:rgaΔ17*

For the removal of the DELLA domain in RGL2, first the *galK* selection marker was introduced between nucleotides 130 to 180 from the ATG. The *galK* was amplified by PCR using oligos RGL2-DELLAGalK-RF and RGL2-DELLAGalK-RR (Supplemental Table S1). These contain a 50 bp region upstream and downstream of the DELLA domain, followed by a short region of the *galK* gene. The PCR was recombined into heat-induced SW102 with the JAtY clone. Colonies were selected on M9 media supplemented with galactose and tested by PCR. Next, two PCR were carried out, using the Accuzyme Taq polymerase, with oligos RGL2-TF1/RGL2-DELLA-RR and RGL2-DELLA-RF/RGL2-TR1. Oligos RGL2-DELLA have complementary ends that, by means of a third PCR using the flaking oligos RGL2-TF1 and RGL2-TR1 and an aliquot of the first two PCRs as template, allows for the generation of a DNA fragment from position -108 to +436 from the ATG of the *RGL2* gene that lacks the DELLA domain (position +130 to +180). The final PCR product was used in a second recombination to replace the *galK*. Colonies lacking the *galK* gene were selected on

deoxy-galactose M9 media. The construct was tested by PCR and sequencing. See supplemental Figure S1B for details.

2.4.3. Construction of *pRGL2:YPet-rgaΔ17* from *pRGL2:rgl2Δ17*

To introduce the YPet protein sequence in the Nt of the rgl2Δ17, the *galK* selection marker was first introduced and then was replaced with the *YPet* gene. A PCR was carried out with recombineering oligos RGL2-Nt_RF and RGL2-Nt_RR using the *galK* cassette as template. This PCR was used for recombination of the construct *pRGL2:rgaΔ17*, and positive colonies were selected on M9 media supplemented with galactose. A second PCR was carried out with Accuzyme Taq polymerase, using the same recombineering oligos and using the *YPet* cassette as template, which also contains the adaptor sequences flanking the ORF. This PCR was used to replace the *galK* by recombination, and positive colonies were selected on M9 media supplemented with deoxygalactose. The construct was tested by PCR and sequencing. See supplemental Figure S1C for details.

2.5. Gene expression analysis by qPCR

Total RNA was extracted using the RNeasy Plant Mini Kit (Qiagen). Genomic DNA was eliminated with 50 units of DNaseI (Qiagen) for 15 min at room temperature. cDNA was synthesized using the SuperScript First-Strand Synthesis System for RT-PCR (Invitrogen). qPCR was carried out using the SYBR® GREEN PCR Master Mix (Applied Biosystems) in an ABI PRISM 7500 Fast Sequence Detection System (Applied Biosystems), essentially as described in Dorcey et al. [20]. Expression levels were calculated relative to the constitutively expressed gene *ubiquitin10* (*UBQ10*, *At4g05320*) [34], which were tested to be constitutive in the different tissues used in

each experiment. Normalization was carried out using the ΔΔCt method (Applied Biosystems), where ΔCt was calculated for each sample as the difference between Ct (gene of interest) and Ct (constitutive gene), and final relative expression level was determined as inverse of $\log_2$ of Ct (sample) – Ct (reference sample). Normalization was as indicated in the figure legends and in the text. Primers used for qPCR were designed with the Primer Express™ v2.0 software (Applied Biosystems) and tested for efficiency (Supplemental Table S1). For the analysis of *YPet-rgl2Δ*17 transgene expression, oligos were designed into the *YPet* sequence (Supplemental Table S1).

2.6. Confocal and Scanning Electron Microscopy (SEM)

A ZEISS LSM 780 confocal microscope was used to detect Venus-RGL2 and YPet-rgl2Δ17. Both proteins were imaged with excitation at 514 nm and emission filters set to 520-540 nm. Endogenous chlorophyll was excited with the same wavelength but detected between 660 and 690 nm. Identity of each signal was confirmed with a λ-scan.

For Scanning Electron Microscopy (SEM), samples were harvested, mounted on the specimen holder of a CT-1000C cryo-transfer system (Oxford Instruments) and frozen in liquid N_2. The frozen samples were transferred to the cryo-stage of a JEOL JSM-5410 scanning electron microscope, sublimated by controlled heating at -85ºC and sputter coated with a thin film of gold. Finally, samples were observed at incident electron energy of 10 keV.

3. Results and Discussion

3.1. *pRGL2:Venus-RGL2* and *pRGL2:YPet-rgl2Δ17* transgenic lines: new genetic tools to study RGL2 function in *Arabidopsis*

To have a deep insight on the role of RGL2 in plant growth and development, and in the absence of *bona-fide* reporter lines of this gene, two transgenic lines that express a Venus-RGL2 fusion protein (*pRGL2:Venus-RGL2*) and a dominant version of RGL2 fused to YPet (*pRGL2:YPet-rgl2Δ17*) were generated, both under the control of the endogenous *RGL2* promoter, using a recombineering strategy (see Supplemental Figure S1A-C and Materials and Methods section for details). The JAtY clone JAtY56P08 containing a large 73 kb *Arabidopsis* genomic DNA fragment that includes the *RGL2* gene (*At3g03450*) was used. The use of the large genomic fragment, which includes all regulatory regions, potentially ensures a veracious expression pattern of the fusion protein, reflecting that of the native gene. In the *pRGL2:YPet-rgl2Δ17* line, a deletion of the DELLA motif (DELLAVLGYKVRSSEMA at position 44-60 of the RGL2 protein) equivalent to those in the *gai-1* mutant [11,35] and in the *pRGA:GFP-rgaΔ17* line [12] was carried out. This DELLA domain deletion was intended to generate a dominant stable version of the RGL2 protein that would not be degraded in the presence of bioactive GAs. Whilst several primary lines were generated, all showing similar plant growth phenotype, two lines were selected and characterized based on morphological phenotype and the expression levels of the *YPet-rgl2Δ*17 transgene (Supplemental Figure S2A-B). One of them, line 15, was selected and used for further assays. Detailed analysis of developmental alterations showed by this dominant line is further described below.

3.2. Venus-RGL2 complements phenotypes of the *quadruple della* mutant.

The *quadruple della* mutant (*gaiT6 rgaT2 rgl1-1 rgl2-1*) shows constitutive GA response, like slender plant phenotype [19], or altered seed shape and size [6]. To confirm that the RGL2-derived protein versions generated truly reflect the expression of the endogenous gene, the *pRGL2:Venus-RGL2* construct was introduced in the *quadruple della* mutant to test whether the phenotypes associated with the GA-constitutive signaling were suppressed. Indeed, the inflorescence morphology and pedicel length, which are the characters altered in the *quadruple della* mutant, were alleviated by the *pRGL2:Venus-RGL2* construct (Supplemental Figure S3A). Moreover, the seed shape and size of the *quadruple della* mutant carrying the *pRGL2:Venus-RGL2* construct were identical to those in wt (Supplemental Figure S3B). On the contrary, expression of *Venus-RGL2* did not suppress the slender phenotype of the *quadruple* mutant (Supplemental Figure S3C). In fact, the plant height is increase in the *quadruple* (*gaiT6 rgaT2 rgl1-1 rgl2-1*) and *triple della* (*gaiT6 rga24 rgl1-1*, with wild-type *RGL2*), but not in other triple *della* mutants (Supplemental Figure S3D), which suggests that RGL2 is not involved in the inflorescence stem elongation. The complementation of pedicel length, inflorescence structure, and seed shape and size in the *pRGL2:Venus-RGL2* line indicate that the Venus-RGL2 fusion protein provides functional RGL2 activity.

3.3. YPet-rgl2Δ17 is a stable GA-resistant protein

Stability of Venus-RGL2 and YPet-rgl2Δ17 fusion proteins were analyzed in primary roots of 4-day-old seedlings, where *RGL2* is expressed (Figure 1A-B). Incubation of seedlings for 24 h in PCB, an inhibitor of GA biosynthesis that causes decreased GA levels, resulted in increased levels of fusion proteins due to stabilization of Venus-RGL2 (Figure 1A). Conversely, Venus-RGL2 protein was degraded when

seedlings were incubated with GAs. Therefore, the *pRGL2:Venus-RGL2* line expressed Venus-RGL2 that behaves as expected for a DELLA protein, was stabilized when GA levels are low or degraded upon elevated GA levels. On the other hand, the stable YPet-rgl2Δ17 protein was not degraded by GAs, as protein levels in the root tip remained constant upon GA treatment (Figure 1B), similar to the widely-used GFP-rgaΔ17 protein [36]. In conclusion, the constructs gendered promote the synthesis of RGL2/rgl2Δ17 proteins that behave as expected in the presence or absence of GAs, and therefore provide a powerful molecular and genetic tool to asset *RGL2* expression and function through plant development.

3.4. YPet-rgl2Δ17 inhibits seed germination

RGL2 protein is known to control GA-mediated seed germination [17,37,38]. For example, in the presence of light, among the DELLA mutants, only *rgl2* is able to germinate when GA levels are low due to either the effect of the GA-deficient mutant *ga1* or upon PCB treatment, which promotes stabilization and accumulation of DELLA proteins [17,18]. More recently, it has been described that the molecular mechanism of RGL2 in the control of seed germination resides in its interaction with the NUCLEAR FACTOR-Y C, which targets ABI5, integrating GA and ABA signaling pathways during germination [39,40]. Therefore, it is expected that the dominant version YPet-rgl2Δ17 should impair germination as it occurs when seeds were challenged to germinate in low GA content. The germination (radicle emergence) of freshly harvested seeds of the wt, the null mutant *rgl2-1*, and dominant *YPet-rgl2Δ17* was monitored. At 72h, *YPet-rgl2Δ17* seeds showed very low germination rate (10%), compared to wt (60%) and the null *rgl2-1* (90%) (Figure 2A). Therefore, *YPet-rgl2Δ17* behaved in terms of germination as expected for a dominant version of RGL2. In fact, seeds of

pRGL2:YPet-rgl2Δ17 required longer times of after- ripening and vernalization to germinate. In agreement with a major role of RGL2 in germination, YPet-rgl2Δ17 was detected in the embryo of freshly harvest seeds of *pRGL2:YPet-rgl2Δ17*, particularly in the axis (hypocotyl, collet, and radicle) (Figure 2B). Previously, the presence of RGL2 was reported in the radicle of young seedlings shortly after seed germination of the *rgl2-5* line [17], a DS-GUS transposon insertion in the *RGL2* ORF. The results of this study, together with previous data, reveal that *RGL2* is expressed in seeds to negatively regulate germination. In freshly harvest seeds, high ABA and low GA levels stabilized RGL2 and hence blocked germination. In the seeds of the *pRGL2:YPet-rgl2Δ17* line, stable *YPet*-rgl2Δ17 protein would repress germination.

3.5. YPet-rgl2Δ17 alters reproductive but not vegetative development

In adult plants, the dominant version of RGL2 caused alterations in flower morphology that ranked from severe in the first flowers in the inflorescence stem to mild in later flowers (Figure 3A-D and Supplemental Figure S2). In contrast, flowering time, plant height, and leaf size and shape were not altered (Figure 3A and Table 1). The absence of alterations in plant architecture in plants expressing the YPet-rgl2Δ17 protein, along with the lack of complementation of the slender phenotype of the *quadruple della* mutant transformed with *pRGL2:Venus-RGL2* (Supplemental Figure S3C), confirmed that RGL2 was not involved in inflorescence stem elongation. This was previously suggested by Lee et al. [17], as they reported that the null mutant *rgl2-1* behaved as the wt in the PCB-inhibition of growth of the inflorescence stem, while null mutants in GAI or RGA did partially recover stem growth, pointing out to a major role of GAI and RGA, but not RGL2, in stem elongation.

Conversely, dominant YPet-rgl2Δ17 promoted the shortening of all four floral whorls, mostly petals and stamen in early flowers (Figures 3C-D and 4A-D). These modifications were attenuated as the inflorescence progresses, although later flowers did not recover normal petal and stamen size (Figure 3C-D and Figure 4G). Moreover, anther dehiscence was also impaired by YPet-rgl2Δ17 (Figure 4C-D). While wt flowers at anthesis showed pollen grains covering the anthers and pistil, equivalent flowers of *pRGL2:YPet-rgl2Δ17* plants developed short filaments and anthers that did not show pollen grains. In agreement with this, it was reported that RGA and RGL2, along with RGL1, repress floral organ development, as the corresponding null mutants were able to alleviate flower development defects, especially anther and pollen development, in the strong GA deficient mutant *ga1-3* [19]. In addition to *ga1*, stamen development was also altered in the dominant *gai-1* or *GFP-rgaΔ17*, which blocked GAI- and RGA-dependent GA signaling, respectively [12,35]. The data in this study indicate that the stable RGL2 activity in *pRGL2:YPet-rgl2Δ17* plants also promotes similar effects in stamen development as those observed in *ga1-3*, *gai-1* or *GFP-rgaΔ17* plants. In any case, further analysis is needed to know whether the arrest of stamen development in these mutants occurs via the same molecular mechanism.

As a consequence of the stamen defects, *pRGL2:YPet-rgl2Δ17* plants showed reduced fertility. Similar to flower morphology alterations, fertility varied throughout the inflorescence. Pistils of early flowers (flower number 5-10) failed to form any seeds, and consequently the valves did not develop into siliques (Figure 3E, right images), while later flowers (flower number 25-30) produced siliques that developed partially (central images) compared to the wt fully developed siliques (left images).

To take a closer look to the fertility phenotype caused by dominant RGL2, we performed a detailed analysis of seed number and silique length in early and late

flowers. In early *pRGL2:YPet-rgl2Δ17* flowers, which show strong reduction of stamen length, the pistils failed to develop into siliques and to form seeds (Figure 5A). In contrast, when these same flowers were pollinated with L*er* pollen, the pistils were able to develop into siliques that contained 60% of the number of seeds in L*er*. In addition, the length of these siliques was only 45% of those in the wt, resulting in an increase in the ratio of seed number to silique length (Figure 5A). This result suggests that YPet-rgl2Δ17 protein partly blocks the elongation of the valve, as the siliques cannot grow proportionally to the number of seeds [41]. Higher ratio of seed to silique length was also described in the double mutant *gid1a gid1c* of the GA receptors GID1 expressed in the valve [42], as valve elongation was compromised due to lack of GA perception. To test whether the short siliques in early flowers of *pRGL2:YPet-rgl2Δ17* plants was due to defects in silique elongation when RGL2-dependent GA signaling was blocked, the response on *pRGL2:YPet-rgl2Δ17* pistils to GA treatment was assayed. As observed in Figure 5C, while L*er* was able to fully respond, forming parthenocarpic fruits that doubled the size of an unfertilized pistil, pistils of the transgenic line only responded partially, suggesting that RGL2 participated in GA-dependent silique elongation (Figure 5C).

Later, during inflorescence development, fertility of *pRGL2:YPet-rgl2Δ17* plants was recovered as the flower phenotype became less severe. Number of seeds of late flowers (flower number 35-40) was similar to wt. In spite of that, these siliques still failed to fully elongate, due to the blockage of valve growth by YPet-rgl2Δ17 (Figure 5B). Moreover, pollination of pistils from late *pRGL2:YPet-rgl2Δ17* flowers with pollen from L*er* resulted in siliques that were identical to those from *YPet-rgl2Δ17* hand-pollinated with *YPet-rgl2Δ17* pollen; these contained similar seed numbers as the L*er*, but were still 10-15% shorter, which caused an increase in the ratio of seed number to

silique length. In contrast, when the reciprocal cross was done, seed number, silique length, and ratio were not altered (Figure 5B). These data indicate that the pistils of L*er* (but not that of *pRGL2:YPet-rgl2Δ17* plants) were fully capable to elongate proportionally to the number of seeds that were developed within, and that the pollen of late flowers of *pRGL2:YPet-rgl2Δ17* plants had no defects. In fact, a direct analysis of pollen germination and pollen tube growth indicate that YPet-rgl2Δ17 did not promote pollen defects in late flowers (Supplemental Table S2), indicating that anther defects observed in early flowers were totally alleviated.

Overall, the data on the floral morphology phenotype in the *pRGL2:YPet-rgl2Δ17* plants obtained in this study suggest a gradient across the inflorescence, with a common trend of alleviation of the phenotypes, including fertility, as the inflorescence stem grows. This trend resembles those described for mutants in the GA biosynthesis genes *GA20oxidase* and *GA3oxidase* [43-46]. Early flowers of double *ga20ox1 ga20ox2* showed a similar shortening of floral organs as the *pRGL2:YPet-rgl2Δ17* plants. Additional combination with mutant *ga20ox3* and *ga20ox4* or *ga20ox5* resulted in further shortening of floral organs, to finally resemble those in the strong GA deficient *ga1-3*. A close analysis of *ga3ox* mutant combinations revealed a strong defect in flower development in the double *ga3ox1 ga3ox3*. More interestingly, the shortening of the floral whorls in this mutant, mainly stamen and petal, was gradually alleviated as new flowers on primary inflorescence developed. Recently, by using mutants of the GA20ox genes, GA-dependent and GA-independent components have been identified in association with changing floral organ growth and development during early inflorescence stem growth [47]. All together, these evidences point out to similar defects in flower development when GA synthesis or GA signaling is limited, especially in flowers developed during early inflorescence stem growth.

3.6. RGL2 positively regulates ovule number

Recently, we have described that GAs negatively module the formation of ovules, being DELLAs a positive factor in ovule number determination [7]. While constitutive GA signaling in the *quadruple della* null mutant or upon GA treatment reduced ovule number, the activity of the stable gai-1 protein promoted the formation of more ovules per pistil, compared to the wt plant. To test whether RGL2 also has a contributive role in ovule number determination, the ovule number in pistils at anthesis of *pRGL2:YPet-rgl2Δ17* plants compared to the wt was determined. Similar to *gai-1*, *pRGL2:YPet-rgl2Δ17* pistils showed a significant 10% increase in ovule number (Figure 5D), which confirms that RGL2 has a positive role in ovule initiation. Interestingly, the increase in ovule number was similar in both early and late flowers. The increased ovule number in *pRGL2:YPet-rgl2Δ17* pistils was consistent with our previous genetic data using null *della* mutants [7]. For example, the *triple della* null mutant in *RGA*, *GAI* and *RGL2* (*gaiT6 rga24 rgl2-1*) showed a similar reduction in ovule number as the *quadruple della* mutant (*gaiT6 rgaT2 rgl1-1 rgl2-1*). Therefore, it was concluded that albeit RGA was the major DELLA involved in ovule number determination, RGL2 along with GAI also played a significant role [7]. Increased ovule number could be due to an indirect effect of increased pistil length. That was not the case of *YPet-rgl2Δ17* plants. While pistil length at anthesis in *pRGL2:YPet-rgl2Δ17* plants did not differ from those in the L*er* (Mock in Figure 5C), ovule number was significantly increased (Figure 5D), indicating that the increase in ovule number by YPet-rgl2Δ17 was independent of ovary length.

Finally, the possibility that the dominant RGL2 caused alteration in seed development was also addressed, as it occurs in the *quadruple della* and *gai-1* [6]. As

can be observed in Figure 4E-F, ovule size and shape were not modified in the *YPet-rgl2Δ17* plants. In contrast, seed size was slightly increased by the expression of the stable YPet-rgl2Δ17 protein (Figure 5D), which suggests that RGL2 also participates in seed development.

3.7. RGL2 protein is localized in floral organs

Expression of *RGL2* has been previously reported in the radicle of germinating seeds and flowers using the DS line *rgl2-5* [17], or by *in situ* mRNA hybridization in placenta and ovule primordia [7]. Analysis using the RGL2-fluorescent lines allowed for the drawing of a map of the localization of RGL2. In addition to the expression in root tip and embryo already described (Figures 1 and 2), expression of *RGL2* (using the *pRGL2:YPet-rgl2Δ17* line) was localized in floral organs, in the placenta and ovules during development, as well as in pollen (Figure 6). YPet-rgl2Δ17 was detected in the filament of stamens and petals (Figure 6A-B), and in the placenta at ovule initiation (Figure 6C-D). Expression was also detected in mature ovules, especially in the funiculus and chalaza (Figure 6E). In pollen, YPet-rgl2Δ17 was detected in the tetrad stage and mature pollen grain (Figure 6F). Therefore, *RGL2* expression pattern fully correlates with the abnormalities in development caused by the expression of *YPet-rgl2Δ17*. Interestingly, no expression of *RGL2* was reported in the inflorescence stem or in leaves [17], which is in agreement with the lack of any abnormalities of the *pRGL2:YPet-rgl2Δ17* plants in plant height or leaf morphology. Overall, localization of RGL2 fully explains the phenotypes observed in the *YPet-rgl2Δ17* line.

In summary, a comprehensive analysis of the role and the expression pattern of RGL2 in *Arabidopsis* have been carried out. To do this, two transgenic lines were

generated and characterized, *Venus-RGL2* and *YPet-rgl2Δ17*, the later encoding a dominant GA-resistant version of RGL2, both under the control of the endogenous regulatory elements of *RGL2*. The data reported here support a key role of RGL2 in flower development, specially petal and stamen. Moreover, RGL2 play a role, along with GAI and RGA, in ovule number.

Declarations of interest

None

Knowledgements

We wish to thank Ms. J. Yun,M.A. Argomániz for technical assistance, and the IBMCP microscopy facility. Edit Syndicate (http://www.editsyndicate.com/) provided proofreading of the manuscript.

Funding

This work was supported by grants from the Spanish Ministry of Economy and Competitiveness-FEDER [BIO2011-26302 and BIO2014-55946] and Generalitat Valenciana [ACOMP/2013/048 and ACOMP/2014/106] to M.A.P-A. and National Science Foundation [MCB-0923727] to J.M.A. MA P-A received a fellowship of the 'Salvador de Madariaga' program from Spanish Ministry of Science and Innovation.

Author contribution

MD.G. performed most of the experiments and analyzed and interpreted data; C.F-A. obtained the transgenic lines and carried out the germination assays; J. O-C. carried out the analysis of plant measurements and flowering time; J.M. A. designed the cloning

strategy for the generation of the transgenic lines; M.A. P-A. conceived the project, carried out the constructs, analyzed and interpreted data, and wrote the article with contributions by all the authors.

4. References

[1] F. Vera-Sirera, M.D. Gomez, M.A.Perez-Amador

DELLA proteins, a group of GRAS transcription regulators, mediate gibberellin signaling, in: D.H. Gonzalez, (Ed.), Plant Transcription Factors: Evolutionary, Structural and Functional Aspects, Elsevier/Academic Press, 2015, pp. 313-328

[2] J.M. Daviere, P. Achard

A pivotal role of DELLAs in regulating multiple hormone signals

Mol. Plant, 9 (2016), pp. 10-20

[3] A. Briones-Moreno, J. Hernandez-Garcia, C. Vargas-Chavez, F.J. Romero-Campero, J.M. Romero, F. Valverde, M.A. Blazquez

Evolutionary analysis of DELLA-associated transcriptional networks

Front. Plant Sci., 8 (2017), pp. 626

[4] T.-p. Sun

The molecular mechanism and evolution of the review GA-GID-DELLA signaling module in plants

Curr. Biol., 21 (2011), pp. 338-345

[5] R. Gupta, S.K. Chakrabarty

Gibberellic acid in plant still a mystery unresolved

Plant Signal. Behav., 8 (2013), pp. e25504

[6] M.D. Gomez, D. Ventimilla, R. Sacristan, M.A. Perez-Amador

Gibberellins negatively regulate ovule integument development by interfering with ATS activity in Arabidopsis

Plant Physiol., 172 (2016), pp. 2403-2415

[7] M.D. Gomez, D. Barro-Trastoy, E. Escoms, M. Saura-Sánchez, I. Sánchez, A. Briones-Moreno, F. Vera-Sirera, E. Carrera, J.J. Ripoll, M.F. Yanofsky, I. Lopez-Diaz, J.M. Alonso, M.A. Perez-Amador

Gibberellins negatively modulate ovule number in plants.

Development, 145 (2018), pp. dev163865

[8] P. Hedden, S.G. Thomas

Gibberellin biosynthesis and its regulation

Biochem. J., 444 (2012), pp. 11-25

[9] J.M. Daviere, P. Achard

Gibberellin signaling in plants

Development, 140, (2013), pp. 1147-1151

[10] P. Hedden, V. Sponsel

A century of gibberellin research

J. Plant Growth Regul., 34 (2015), pp. 740-760

[11] J. Peng, P. Carol, D.E. Richards, K.E. King, R.J. Cowling, G.P. Murphy, N.P. Harberd

The Arabidopsis GAI gene defines a signaling pathway that negatively regulates gibberellin responses

Genes Dev., 11 (1997), pp. 3194-205

[12] A. Dill, H.S. Jung, T.-p. Sun

The DELLA motif is essential for gibberellin-induced degradation of RGA

Proc. Natl. Acad. Sci. USA, 98 (2001), pp. 14162-14167

[13] A.L.Silverstone, P.Y. Mak, E.C. Martinez, T.-p. Sun

The new RGA locus encodes a negative regulator of gibberellin response in *Arabidopsis thaliana*

Genetics, 146 (1997), pp. 1087-1099

[14] A.L. Silverstone, C.N. Ciampaglio, T-p. Sun

The Arabidopsis RGA gene encodes a transcriptional regulator repressing the gibberellin signal transduction pathway

Plant Cell, 10 (1998), pp. 155-169

[15] K.E. King, T. Moritz, N.P. Harberd

Gibberellins are not required for normal stem growth in *Arabidopsis thaliana* in the absence of GAI and RGA

Genetics, 159 (2001), pp. 767-776

[16] A. Dill, T.-p. Sun

Synergistic derepression of gibberellin signaling by removing RGA and GAI function in *Arabidopsis thaliana*

Genetics, 159 (2001), pp. 777-785

[17] S. Lee, H. Cheng, K.E. King, W. Wang, Y. He, A. Hussain, J. Lo, N.P. Harberd, J. Peng

Gibberellin regulates Arabidopsis seed germination via RGL2, a GAI/RGA-like gene whose expression is up-regulated following imbibition

Genes Develop., 16 (2002), pp. 646-658

[18] L. Tyler, S.G. Thomas, J. Hu, A. Dill, J.M.Alonso, J.R. Ecker, T.-p. Sun

DELLA proteins and gibberellin-regulated seed germination and floral development in Arabidopsis

Plant Physiol., 135 (2004), pp. 1008-1019

[19] H. Cheng, L. Qin, S. Lee, X. Fu, D.E. Richards, D. Cao, D. Luo, N.P. Harberd, J. Peng

Gibberellin regulates Arabidopsis floral development via suppression of DELLA protein function

Development, 131 (2004), pp. 1055-1064

[20] E. Dorcey, C. Urbez, M.A. Blazquez, J. Carbonell, M.A. Perez-Amador

Fertilization-dependent auxin response in ovules triggers fruit development through the modulation of gibberellin metabolism in *Arabidopsis*.

Plant J., 58 (2009), pp. 318-332

[21] S. Fuentes, K. Ljung, K. Sorefan, E. Alvey, N.P. Harberd, L. Ostergaard

Fruit growth in Arabidopsis occurs via DELLA-dependent and DELLA-independent gibberellin responses

Plant Cell, 24 (2012), pp. 3982-3996

[22] M. Wild, P. Achard

The DELLA protein RGL3 positively contributes to jasmonate/ethylene defense responses

Plant Signal Behav., 8 (2013), pp. e23891

[23] M. Wild, J.M. Davière, S. Cheminant, T. Regnault, N. Baumberger, D. Heintz, R. Baltz, P.Genschik, P. Achard

The Arabidopsis DELLA RGA-LIKE3 is a direct target of MYC2 and modulates jasmonate signaling responses

Plant Cell, 24 (2012), pp. 3307-3319

[24] J. Gallego-Bartolome, E.G. Minguet, J.A. Marin, S. Prat, M.A. Blazquez, D. Alabadi

Transcriptional diversification and functional conservation between DELLA proteins in Arabidopsis

Mol. Biol. Evol., 27 (2010), pp. 1247-1256

[25] P. Stamm, P. Ravindran, B. Mohanty, E.L. Tan, H. Yu, P.P. Kumar

Insights into the molecular mechanism of RGL2-mediated inhibition of seed germination in *Arabidopsis thaliana*

BMC Plant Biol., 12 (2012), pp. 179

[26] T. Murashige, F. Skoog

A revised medium for rapid growth and bioassays with tobacco tissue cultures

Physiol. Plant, 15 (1962), pp. 473-497

[27] M.D. Abramoff, P.J. Magelhaes, S.J. Ram

Image processing with ImageJ

Biophot. Int., 11 (2004), pp. 36-42

[28] B. Tursun, L.Cochella, I. Carrera, O. Hobert

A toolkit and robust pipeline for the generation of fosmid- based reporter genes in *C. elegans*

PLoS ONE, 4 (2009), pp. e4625

[29] N.G. Copeland, N.A. Jenkins, D.L. Court

Recombineering: a powerful new tool for mouse functional genomics

Nat. Rev. Genet., 2 (2001), pp. 769-779

[30] S. Warming, N. Costantino, D.L. Court, N.A. Jenkins, N.G. Copeland

Simple and highly efficient BAC recombineering using galK selection

Nucleic Acids Res., 33 (2005), pp. e36

[31] R. Zhou, L.M. Benavente, A.N. Stepanova, J.M. Alonso

A recombineering-based gene tagging system for Arabidopsis

Plant J., 66 (2011), pp. 712-723

[32] Y.G. Liu, H. Liu, L. Chen, W. Qiu, Q. Zhang, H. Wu, C. Yang, J. Su, Z. Wang, D. Tian, M. Mei

Development of new transformation-competent artificial chromosome vectors and rice genomic libraries for efficient gene cloning

Gene, 282 (2002), pp. 247-255

[33] S.J. Clough, A.F. Bent

Floral dip: a simplified method for Agrobacterium-mediated transformation of *Arabidopsis thaliana*

Plant J., 16 (1998), pp. 735-743

[34] T. Czechowski, M. Stitt, T. Altmann, M.K. Udvardi, W.R. Scheible

Genome-wide identification and testing of superior reference genes for transcript normalization in Arabidopsis

Plant Physiol., 139 (2005), pp. 5-17

[35] M. Koorneef, A. Elgersma, C.J. Hanhart, E.P. van Loenen-Martinet, L. van Rijn, J.A.D. Zeevaart

A gibberellin insensitive mutant of *Arabidopsis thaliana*

Physiol. Plant., 65 (1985), pp. 33-39

[36] A.L. Silverstone, H.S. Jung, A. Dill, H. Kawaide, Y. Kamiya, T.-p. Sun

Repressing a repressor: gibberellin-induced rapid reduction of the RGA protein in Arabidopsis

Plant Cell, 13 (2001), pp. 1555-1566

[37] K.P. Lee, U. Piskurewicz, V. Tureckova, M. Strnad, L. Lopez-Molina

A seed coat bedding assay shows that RGL2-dependent release of abscisic acid by the endosperm controls embryo growth in Arabidopsis dormant seeds

Proc. Natl. Acad. Sci. USA, 107 (2010), pp. 19108-19113

[38] J. Peng, N.P. Harberd

The role of GA-mediated signalling in the control of seed germination

Curr. Opin. Plant Biol., 5 (2002), pp. 376-381

[39] X. Liu, P. Hu, M. Huang, Y. Tang, Y. Li, L. Li, X. Hou

The NF-YC-RGL2 module integrates GA and ABA signalling to regulate seed germination in Arabidopsis

Nat. Commun., 7 (2016), pp. 12768

[40] D. Jin, M. Wu, B. Li, B. Bücker, P. Keil, S. Zhang, J. Li, D. Kang, J. Liu, J. Dong, X.W. Deng, V. Irish, N. Wei

The COP9 Signalosome regulates seed germination by facilitating protein degradation of RGL2 and ABI5

PLoS Genet., 14 (2018), pp. e1007237

[41] C.M. Cox, S.M. Swain

Localised and non-localised promotion of fruit development by seeds in Arabidopsis

Func. Plant Biol., 33 (2006), pp. 1-8

[42] C. Gallego-Giraldo, J. Hu, C. Urbez, M.D. Gomez, T.-p. Sun, M.A. Perez-Amador

Role of the gibberellin receptors GID1 during fruit-set in Arabidopsis

Plant J., 79 (2014), pp. 1020-1032

[43] J. Hu, M.G. Mitchum, N. Barnaby, B.T. Ayele, M. Ogawa, E. Nam, W.C. Lai, A. Hanada, J.M. Alonso, J.R. Ecker, S.M. Swain, S. Yamaguchi, Y. Kamiya, T.-p. Sun

Potential sites of bioactive gibberellin production during reproductive growth in Arabidopsis

Plant Cell, 20 (2008), pp. 320-336

[44] I. Rieu O. Ruiz-Rivero, N. Fernandez-Garcia, J. Griffiths, S.J. Powers, F. Gong, T. Linhartova, S. Eriksson, O. Nilsson, S.G. Thomas, A.L. Phillips, P. Hedden

The gibberellin biosynthetic genes *AtGA20ox1* and *AtGA20ox2* act, partially redundantly, to promote growth and development throughout the Arabidopsis life cycle

Plant J., 53 (2008), pp. 488-504

[45] A.R.G. Plackett, S.G. Thomas, Z.A. Wilson, P. Hedden

Gibberellin control of stamen development: a fertile field

Trends Plant Sci., 16 (2011), pp. 568-578

[46] A.R.G. Plackett, S.J. Powers, N. Fernandez-Garcia, T. Urbanova, Y. Takebayashi, M. Seo, Y. Jikumaru, R. Benlloch, O. Nilsson, O. Ruiz-Rivero, A.L. Phillips, Z.A. Wilson, S.G. Thomas, P. Hedden

Analysis of the developmental roles of the Arabidopsis gibberellin 20-oxidases demonstrates that GA20ox1, -2, and -3 are the dominant paralogs.

Plant Cell, 24 (2012), pp. 941-960

[47] A.R.G. Plackett, S.J. Powers, A.L. Phillips, Z.A. Wilson, P. Hedden, S.G. Thomas

The early inflorescence of *Arabidopsis thaliana* demonstrates positional effects in floral organ growth and meristem patterning

Plant Reprod., 31 (2017), pp. 171-191

[48] C. Ferrandiz, S. Pelaz M.F. Yanofsky

Control of carpel and fruit development in Arabidopsis

Annu. Rev. Biochem., 68 (1999), pp. 321-354

Figure Legends

Figure 1. Expression and stability of RGL2 and rgl2Δ17 monitored in transgenic lines *pRGL2:Venus-RGL2* (A) and *pRGL2:YPet-rgl2Δ17* (B). A, Venus-RGL2 is localized in the roots of 4-days old seedlings (Mock, middle panel), but it is degraded in the presence of 1 µM GA_{4+7} (+GA, left panel), or stabilized in the presence of 1 µM PCB (+PCB, right panel). **B**, Deletion of the DELLA domain in RGL2 promotes the YPet-rgl2Δ17 protein to be resistant to GA-induced degradation. YPet-rgl2Δ17, GFP-rgaΔ17, and GFP-RGA proteins in transgenic lines *pRGL2:YPet-rgl2Δ17*, *pRGA:GFP-rgaΔ17* [12], and *pRGA:GFP-RGA* [36], respectively, in the primary root of 4-days old seedlings in the absence (Mock, upper panels) or presence of 1 and 3 µM GA_{4+7} (+GA, middle or bottom panels). Scale bars represent 20 µm.

Figure 1

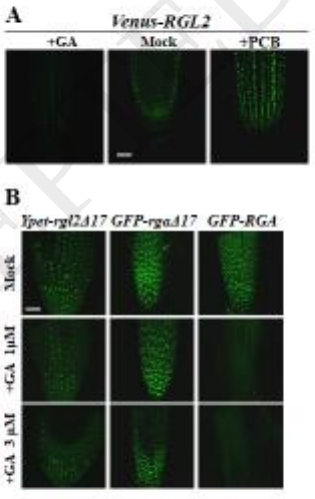

Figure 2. YPet-rgl2Δ17 inhibits seed germination. A, Seeds of the *pRGL2:YPet-rgl2Δ17* line show reduced germination, compared to the wt and the null mutant *rgl2-1*. Percentage of germination of freshly harvested seeds four days after incubation in MS at 22°C. Mean and SD were calculated in triplicate, from at least 80 seeds per each line and biological replica. Significant differences (Student's *t*-test analysis) with wt are marked with asterisk (*, p-value <0.01). **B,** expression of YPet-rgl2Δ17 in the embryo of a freshly harvest seed of *pRGL2:YPet-rgl2Δ17*. Seed coat was mechanically removed after imbibition for 24h at 4°C. Hyp, hypocotyl; Col, collet; Cot, cotyledon; Rad, radicle. Scale bar represents 100 µm.

Figure 2

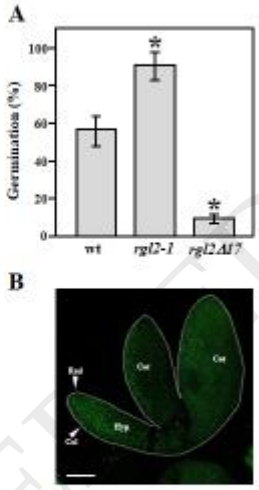

Figure 3. YPet-rgl2Δ17 promotes alterations in flowers and fruits but does not affect plant height. Images of wt and *pRGL2:YPet-rgl2Δ17* whole plants **(A),**

inflorescences in lateral **(B)** or zenithal **(C)** view, flowers at anthesis **(D)**, and mature fruits **(E)**. In C, D and E, right and middle images represents flowers or fruits developed early or late in the main inflorescence, respectively, of *pRGL2:YPet-rgl2Δ17* plants. Scale bars represent 1 mm.

Figure 3

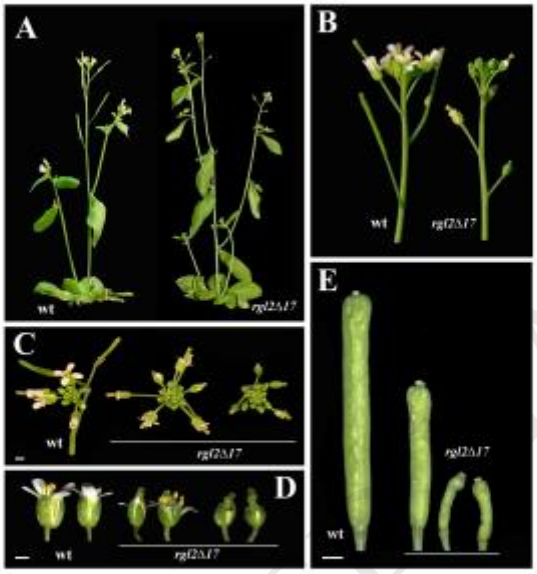

Figure 4. YPet-rgl2Δ17 promotes shortening of the four floral whorls. **A-F,** SEM images of flowers from the wt (A, C, and E) and *YPet-rgl2Δ17* plants (B, D, and F) at one day before anthesis (A and B), flowers at anthesis (C and D), and in ovules at anthesis (E and F). Scale bars represent 500 µm in A to D, and 50 µm in E and F. **G,** length of sepal, petal, stamen, and pistil in early (light grey) or late (dark grey) flowers of *YPet-rgl2Δ17* plants. Data are the percentage of organ length compared to wt (100%), and are the mean±SE of three independent experiments, each one from 20-30

flowers per genotype. Significant differences (Student's *t*-test analysis) with wt are marked with asterisks (* p-value < 0.01).

Figure 4

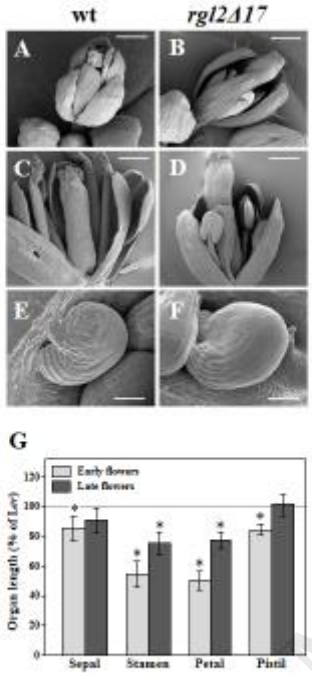

Figure 5. Fertility is compromised by YPet-rgl2Δ17. **A,** Maternal and paternal defects of early flowers (flower number 1-10 in main inflorescence) of *YPet-rgl2Δ17* plants. **B,** Maternal and paternal defects of late flowers (flower number 20-30 in main inflorescence) of *YPet-rgl2Δ17* plants. In A and B, data are shown as percentages of fruit length, seed number and the ratio of seed number to fruit length from L*er* and *YPet-rgl2Δ17* flowers emasculated and pollinated with pollen from L*er* or *YPet-rgl2Δ17* plants. Data were calculated from at least 50 pistils/fruits per treatment. **C,** GA response of unfertilized pistils of wt and *YPet-rgl2Δ17* plants. **D,** Ovule number per pistils in

flowers at anthesis and mature seed length of wt and *YPet-rgl2Δ17* plants. In A-D, data are shown as percentage to wt, and significant differences (Student's *t*-test analysis) between wt and *YPet-rgl2Δ17* are marked with asterisk (*, p-value <0.01).

Figure 5

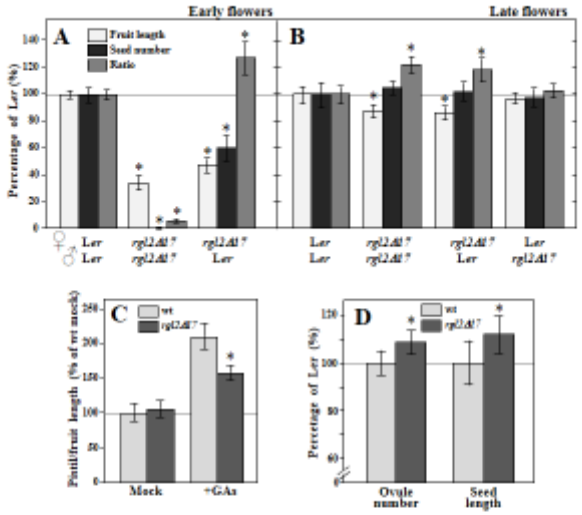

Figure 6. RGL2 is expressed in floral whorls, ovules and pollen. Expression of YPet-rgl2Δ17 in the filament of the stamen **(A)** and petal **(B)**, the placenta of pistils at stage 8 (**C**) and 9 (**D**) of development [48], in the funiculus and chalaza of mature ovules **(E)** and in pollen grains **(F)**. Inset in F represent YPet-rgl2Δ17 expression in the tetrad stage of pollen development. Ant, anther; Ch, ovule chalaza; F; ovule funiculus; Fil, filament of the stamen; Ov, ovule; Pet, petal; Pl, placenta. Scale bars represent 50 µm in A-D and 30 µm in E-F.

Figure 6

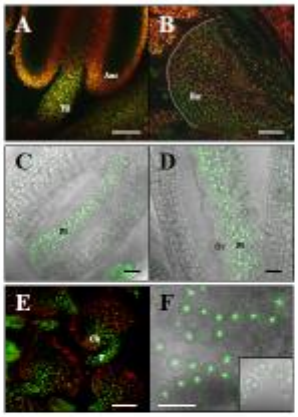

Table I. YPet-rgl2Δ17 does not affect flowering time or plant height

	Flowering time (leaf number)				Plant height (cm)	
	LD		SD			
	Mean	SE	Mean	SE	Mean	SE
Ler	6.8	0.2	16.5	0.9	21.5	2.9
rgl2Δ17	6.7[1]	0.3	16.2*	0.5	20.5[1]	1.9

SD, short-day photoperiod (8/16 h light/dark).

[1], Non-significant differences (Student's t-test analysis; p-value > 0.01).

LD, long- day photoperiod (16/8 h light/dark).